Published in final edited form as:
J Pharmacol Exp Ther. 2008 February ; 324(2): 484–496. doi:10.1124/jpet.107.129890.

Novel Analogs and Stereoisomers of the Marine Toxin Neodysiherbaine with Specificity for Kainate Receptors

L. Leanne Lash, **James M. Sanders**, **Nobuyuki Akiyama**, **Muneo Shoji**, **Pekka Postila**, **Olli T. Pentikäinen**, **Makoto Sasaki**, **Ryuichi Sakai**, and **Geoffrey T. Swanson**
Department of Pharmacology and Toxicology, University of Texas Medical Branch, Galveston, Texas (L.L.L., J.M.S.); Department of Molecular Pharmacology and Biological Chemistry, Northwestern University Feinberg School of Medicine, Chicago, Illinois (L.L.L., G.T.S.); Laboratory of Biostructural Chemistry, Graduate School of Life Sciences, Tohoku University, Sendai, Japan (N.A., Mu.S., Ma.S.); Nanoscience Center and Department of Biological and Environmental Science, University of Jyvaäskylaä, Jyvaäskylaä, Finland (P.P., O.T.P.); and School of Fisheries Sciences, Kitasato University, Iwate, Japan (R.S.)

Abstract

Antagonists for kainate receptors (KARs), a family of glutamate-gated ion channels, are efficacious in a number of animal models of neuropathologies, including epilepsy, migraine pain, and anxiety. To produce molecules with novel selectivities for kainate receptors, we generated three sets of analogs related to the natural marine convulsant neodysiherbaine (neoDH), and we characterized their pharmacological profiles. Radioligand displacement assays with recombinant α-amino-3-hydroxy-5-methyl-4-isoxazolepropionic acid (AMPA) and KARs demonstrated that functional groups at two positions on the neoDH molecule are critical pharmacological determinants; only binding to the glutamate receptor (GluR)5-2a subunit was relatively insensitive to structural modifications of the critical functional groups. NeoDH analogs in which the L-glutamate congener was disrupted by epimerization retained low affinity for GluR5-2a and GluR6a KAR subunits. Most of the analogs showed agonist activity in electrophysiological recordings from human embryonic kidney-T/17 cells expressing GluR5-2a KARs, similar to the natural convulsant neoDH. In contrast, 2,4-epi-neoDH inhibited glutamate currents evoked from both GluR5-2a and GluR6a receptor-expressing cells. Therefore, this compound represents the first compound to exhibit functional antagonist activity on GluR5-2a and GluR6a KAR subunits without concurrent activity on AMPA receptor subunits. Finally, binding affinity of the synthetic ligands for the GluR5-2a subunit closely correlated with their seizurogenic potency, strongly supporting a role for receptors containing this subunit in the convulsant reaction to KAR agonists. The analogs described here offer further insight into structural determinants of ligand selectivity for KARs and potentially represent useful pharmacological tools for studying the role of KARs in synaptic physiology and pathology.

Kainate receptors (KARs) are a family of ionotropic glutamate receptors that play a variety of roles in the mammalian brain. They contribute to excitatory postsynaptic transmission at some synapses, modulate excitatory and inhibitory neurotransmission from presynaptic loci, and modify network excitability through actions on neuronal ion channels (for reviews, see Lerma, 2006; Pinheiro and Mulle, 2006). Targeting KARs could be a useful strategy for therapy in several neurological diseases because antagonists are efficacious in animal models of epilepsy

Address correspondence to: Dr. Geoffrey T. Swanson, Department of Molecular Pharmacology and Biological Chemistry, Northwestern University Feinberg School of Medicine, 303 E. Chicago Ave., Chicago, IL 60611. gtswanson@northwestern.edu.

(Smolders et al., 2002), neuropathic and migraine pain (Filla et al., 2002; Weiss et al., 2006), and anxiety (Alt et al., 2007).

Successful manipulation of neuronal KARs, which are selectively targeted and have distinct subunit stoichiometries, will require expansion of the existing set of pharmacological agents. KAR subunits assemble to form tetrameric channels composed of the obligate GluR5, GluR6, or GluR7 subunits alone or in heteromeric combination with KA1 and KA2 subunits, which do not form functional homomeric receptors (Werner et al., 1991; Herb et al., 1992; Hollmann and Heinemann, 1994). At present, the majority of KAR antagonists and agonists with any degree of selectivity target receptors containing the GluR5 subunit. Furthermore, no compounds exist that broadly inhibit KARs (of all stoichiometries) without also antagonizing AMPARs (Kew and Kemp, 2005). For example, substitution at the 5-position of the uracil ring of N^3-substituted willardiine derivatives generates potent and selective GluR5 KAR antagonists (Dolman et al., 2007). Noncompetitive antagonists also exist for GluR5-containing receptors (Valgeirsson et al., 2003; Christensen et al., 2004; Valgeirsson et al., 2004). A GluR6 antagonist has been described, but this compound, NS-102, has seen only limited use because of insolubility and questions regarding its subuwnit selectivity (Paternain et al., 1996; Lerma et al., 2001). Thus, there remains a compelling need for the development of ligands with a larger spectrum of specificity for KAR subunits and general KAR antagonists without activity at AMPARs.

Toward that end, we have been interested in natural source compounds as tools to probe KAR function at the structural level and in neurotransmission. We previously showed that dysiherbaine (DH), a marine toxin from the sponge *Dysidea herbacea*, is a high-affinity, subunit-selective KAR agonist and consequently a potent convulsant (Sakai et al., 1997, 2001b). DH shares a glutamate congener with other KAR agonists such as kainate and domoate, but it is distinct in that it contains a tetra-substituted hydrofuropyran ring system with two functional groups, at the C8 and C9 positions, that largely control selectivity for AMPA and kainate receptors (Sasaki et al., 1999; Sakai et al., 2001a). Further characterization of a natural analog of DH, neodysiherbaine (neoDH), and a C8/C9 dideoxy synthetic analog of DH, MSVIII-19, revealed that slight structural modifications cause significant changes in the pharmacological activity, including generation of a functional antagonist for GluR5-containing receptors in MSVIII-19 (Sasaki et al., 1999; Sakai et al., 2001a; Sanders et al., 2005).

To determine how additional modification of the template structure could alter activity on KARs, new analogs of neoDH were synthesized and characterized using radioligand binding assays and patch-clamp analysis in this study. First, the C8 and C9 hydroxyl groups were removed individually (deoxy analogs) to generate the intermediate analogs between neoDH and MSVIII-19. In a second set of analogs, the stereochemistry of the C8 and C9 hydroxyl groups was reversed both individually and concurrently. Finally, a third set of analogs with altered chirality of the C2 and C4 carbons were tested for activity; these compounds were generated as by-products of the total synthesis of neoDH previously, and they were significantly less seizurogenic than the parent neoDH compound (Shoji et al., 2006). To elucidate analog binding and specificity at the atomic level, we carried out molecular dynamic simulations for the ligand-binding domain of the GluR5 KAR subunit with docked ligands. Our data demonstrate that the spatial orientation of the C8 and C9 functional groups in the neoDH molecule also are critical determinants of pharmacological activity and that structural modification within the glutamate congener offers potential for the generation of compounds with novel pharmacological profiles on KARs. We also found a high degree of correlation between the binding affinity for the GluR5-2a subunit and seizurogenic potency of the analogs, supporting a central role for receptors containing this subunit in induction of convulsions.

Materials and Methods

Cell Culture and Electrophysiology

HEK-293-T/17 cells were maintained in Dulbecco's modified Eagle's medium supplemented with 100 μg/ml penicillin, 100 μg/ml streptomycin, and 10% heat-inactivated fetal bovine serum. One day before transfection, HEK-T/17 cells were plated at low density on glass coverslips coated with 100 μg/ml poly-D-lysine and 100 μg/ml collagen. Cells were transfected with receptor cDNAs (0.05–0.2 μg) in combination with enhanced green fluorescent protein cDNA for visualization of transfected cells. Transfections were carried out with FuGENE6 (Roche Applied Science, Indianapolis, IN) according to the manufacturer's protocol, and they were used 2 to 3 days after transfection. Internal solution consisted of 110 mM CsF, 30 mM CsCl, 4 mM NaCl, 0.5 mM $CaCl_2$, 10 mM HEPES, and 5 mM EGTA, and it was adjusted to pH 7.3 with CsOH. The external solution contained 150 mM NaCl, 2.8 mM KCl, 2 mM $CaCl_2$, 1 mM $MgCl_2$, and 10 mM HEPES, adjusted to pH 7.3 with NaOH. Patch electrodes from thick-walled borosilicate glass (Warner Instruments, Hamden, CT) were pulled to a final resistance of 1.5 to 2.5 MΩ after fire polishing. Drugs were applied with fast application through a three-barrel glass tube mounted on a piezo-bimorph; glutamate-evoked currents from transfected cells lifted into the laminar solution flow had a 10 to 90% rise-time of 0.8 to 1.5 ms (Swanson et al., 1997). Several drug reservoirs fed into each glass barrel through manifolds, and these had an effective exchange rate between drug solutions of ~1 min. To determine the pre-desensitization IC_{50} values of selected analogs, several control glutamate (10 mM) applications were followed by a 2.5-min application of various concentrations of 8-deoxy-neoDH, 9-deoxy-neoDH, or MSVIII-19, after which the analogs were coapplied with glutamate. A similar protocol was followed to measure the recovery of glutamate-evoked currents, with the exception that the analogs were not coapplied with glutamate. Whole-cell patch-clamp recordings were carried out using an Axopatch 200B amplifier (Axon Instruments, Foster City, CA). Data were analyzed with Origin 7.5 (OriginLab Corp., Northampton, MA), and Prism 4 (GraphPad Software Inc., San Diego, CA); inhibition-response curves were plotted and fit with a one-site competition curve constrained to fixed minima (0) and maxima (100).

Materials

Analogs of neoDH were synthesized as described previously (Shoji et al., 2006), and they were dissolved in double-distilled H_2O.

Modeling and Molecular Dynamics Simulations

The ligand molecules were sketched with SYBYL 7.3 (Tripos, St. Louis, MO), optimized quantum mechanically with Gaussian03 (Frisch et al., 2004), and docked flexibly with Gold 2.2 (Jones et al., 1997) into both ligand binding sites of the three-dimensional structure of the iGluR5 with bound (*S*)-glutamate (Protein Data Bank access code 1YCJ) (Naur et al., 2005). The initiation of protein-ligand complexes for molecular dynamics (MD) simulations were done as described previously (Pentikäinen et al., 2006). Energy minimizations and MD simulations were performed with NAMD 2.6 (Phillips et al., 2005). Initialization and equilibration of the system were done as described previously (Pentikäinen et al., 2007). The production simulations were run for 2.1 to 15 ns at constant temperature of 300 K and at constant pressure of 1 atmosphere. Longer simulations were performed for some ligands to ensure that the protein-ligand complexes were stable. The MD trajectories were analyzed with ptraj6.5. Snapshots at the 1.5-ns time point were selected for figures because they represent well the protein-ligand conformations for all studied complexes.

Radioligand Binding

Membrane preparations from HEK-293-T/17 cells were prepared and used in radioligand binding assays as described previously (Sanders et al., 2005). Unlabeled analogs were used to displace [^{3}H]kainate (10–20 nM; PerkinElmer Life and Analytical Sciences, Boston, MA) or [^{3}H]AMPA (20 nM; PerkinElmer Life and Analytical Sciences) from KARs and AMPARs, respectively. Nonspecific binding was determined in the presence of 1 mM glutamate. After 1-h incubation at 4°C, samples were harvested by rapid filtration onto Whatman GF/C membranes. Upon addition of scintillation fluid, membranes were incubated for1hat room temperature. A Beckman LS5000TD scintillation counter was used for quantification (Beckman Coulter Inc., Fullerton, CA). K_i values were calculated with the Cheng-Prusoff equation using the determined IC_{50} values and the radioligand K_d value. Data were plotted and fit with a one-site competition curve with fixed minima (0) and maxima (100) (Prism 4). Correlation analysis was performed with these binding data and the seizure activity of each analog, represented as ED_{50} values.

Results

To characterize the molecular determinants of selectivity and specificity of KAR ligands that are structurally related to the marine convulsant neoDH, we synthesized representatives of three types of analogs (Fig. 1). Group 1 analogs lack the hydroxyl group additions at the C8 and C9 ring positions that were previously identified as important determinants of pharmacological activity and selectivity (Sanders et al., 2006); therefore, they represent intermediates between the natural dihydroxyl high-affinity agonist neoDH and the dideoxy synthetic analog MSVIII-19, which acts as a selective GluR5 antagonist (Sanders et al., 2005). The other groups consist of stereoisomeric analogs designed to test the importance of the spatial orientation of the C8 and C9 hydroxyl moieties (group 2) and the C2 and C4 carbons within the L-glutamate congener of the parent molecule (group 3) (Shoji et al., 2006).

Deoxy Analogs Retain Affinity and Agonist Activity on GluR5 KAR Subunits

The pharmacological profiles of the group 1 analogs 8-deoxy-neoDH and 9-deoxy-neoDH were analyzed initially in radioligand binding experiments with expressed recombinant AMPA and kainate receptor subunits. Displacement of [^{3}H]kainate from cell membranes with a range of analog concentrations yielded IC_{50} values that were then used to calculate K_i values for each analog/receptor combination. Both group 1 analogs retained high affinity only for GluR5-2a KAR subunits (Fig. 2A). The binding affinity of 8-deoxy-neoDH for GluR5-2a subunits (K_i = 1.5 nM; n = 3–5) was higher than that of the parent compound neoDH (K_i = 7.7 nM; Sanders et al., 2005). Because the subunit isoform of GluR5 that is predominantly expressed in the brain is GluR5-2b, we repeated radioligand binding assays with 8-deoxy-neoDH on GluR5-2b subunits, and we found no substantial change in affinity [K_i = 2.0 nM (n = 3–5) versus 1.5 nM for GluR5-2a subunits]. Weak binding to other KAR and AMPAR subunits was observed, with all K_i values estimated at >10 μM(n = 3–5; Table 1;Fig. 2A). K_i values calculated from the displacement curves for each analog on each receptor subunit are shown in Table 1. For comparison, the K_i values for neoDH and MSVIII-19 are included in the table (Sanders et al., 2005). Removal of the C9 hydroxyl eliminated binding to all receptor subunits (K_i values estimated at >100 μM), with the exception of GluR5-2a KARs. 9-Deoxy-neoDH displaced radioligand from these receptors, with a K_i of 169 nM (n = 3–4; Fig. 2A), which is quite similar to that observed with MSVIII-19, the dideoxy analog that acts as an antagonist. These data suggest that loss of the substituent at the C9 position largely underlies the difference in binding affinity between neoDH and MSVIII-19.

Because neoDH and its natural analog, DH, both act as KAR agonists, we tested each of the analogs for agonist activity using whole-cell patch-clamp recordings. Application of saturating

concentrations of glutamate (10 mM) to a transiently transfected HEK-293-T/17 cell was first done to obtain a rapidly activating and desensitizing control current; this was then followed by a test application of the analog at a high concentration (10–100 μM). Both 8-deoxy-neoDH (100 μM) and 9-deoxy-neoDH (100 μM) elicited currents from GluR5-2a receptors (n = 3–4; Fig. 2B), confirming that these compounds are KAR agonists. 8-Deoxy-neoDH is probably a full agonist, or a highly efficacious partial agonist, because the amplitude of currents elicited from GluR5 receptors at a concentration of 100 μM were similar to those evoked by saturating concentrations of glutamate. In contrast, 9-deoxy-neoDH was a very weak agonist that evoked only small currents at high concentrations.

9-Deoxy-neoDH and the dideoxy antagonist MSVIII-19 have very similar binding profiles on GluR5-2a and other subunits (Sanders et al., 2005), but both their functional activities and behavioral properties differ. 9-Deoxy-neoDH elicits small but reproducible currents from GluR5-2a receptors (Fig. 2B), whereas MSVIII-19 behaves as an antagonist (Sanders et al., 2005). To further compare the activity of these compounds and the high-affinity agonist 8-deoxy-neoDH on GluR5-2a receptors, we determined their respective IC_{50} values for pre-desensitization of the receptor (Fig. 3). Responses to 10 mM glutamate were elicited to determine the control current amplitudes for GluR5-2a-expressing cells; receptors were then pre-desensitized with low concentrations of the analog (8-deoxy-neoDH or 9-deoxy-neoDH) before test coapplications with glutamate. Figure 3A shows representative control and test traces in which preapplication of 1 μM 8-deoxy-neoDH completely inhibited a glutamate-evoked current from a GluR5-2a-expressing cell. In contrast, 1 μM 9-deoxy-neoDH inhibited, but it did not abolish glutamate-evoked currents. Pre-desensitization of GluR5-2a receptors occurred in a concentration-dependent manner, as shown in Fig. 3B, which also contains our previous data from similar experiments with MSVIII-19 for comparative purposes (Sanders et al., 2005). Inhibition-response analysis yielded an IC_{50} value of 151 nM for 9-deoxy-neoDH inhibition of GluR5-2a receptor activation (n = 3; Fig. 3B). This is a similar but somewhat less potent inhibitory activity than MSVIII-19, which has an IC_{50} on GluR5-2a receptors of 23 nM (Sanders et al., 2005). 8-deoxy-neoDH inhibited GluR5-2a receptor activation more potently, with an IC_{50} value of 238 pM (n = 3–4).

Several analogs, including the parent compounds DH and neoDH, induce a very stable, ligand-bound desensitized conformation of GluR5-2a and GluR6a receptors that occludes subsequent activation of the receptors for long periods. We measured the duration of the interaction of group I analogs with GluR5-2a receptors by determining the time course of recovery of glutamate-evoked currents after application of the analogs (for ~2.5 min) (Fig. 4). In Fig. 4A, traces on the left are representative control glutamate-evoked currents; traces on the right are glutamate-evoked currents 10 min after exposure to 8-deoxy-neoDH, 9-deoxy-neoDH, or MSVIII-19 (each at 30 μM). The high-affinity agonist 8-deoxy-neoDH completely attenuated glutamate currents in response to glutamate for up to 15 min (n = 3; Fig. 4B), similar to both DH and neoDH (Swanson et al., 1997;Sanders et al., 2005). In contrast, glutamate elicited large-amplitude currents relatively rapidly after application of either 9-deoxy-neoDH (time constant for recovery, τ = 1.5 s; n = 3–5) or MSVIII-19 (τ = 1.4 s; n = 3–6); in both cases, the currents returned to an equilibrium amplitudes in ~3 min. It should be noted that GluR5-2a receptors exhibit significant run-down in current amplitudes under normal conditions, without analog application, to ~75 to 80% of control within 10 min of initiation of whole-cell recording (n = 9; Fig. 8). It is not clear whether the degree of attenuation of glutamate currents after 9-deoxy-neoDH, which seems somewhat lower than is accountable for simply by run-down of currents, represents stable binding with a subset of subunits within the tetrameric GluR5-2a receptor, or whether it reflects variability in the degree of run-down during those particular recordings. Regardless, these data demonstrate that 9-deoxy-neoDH and MSVIII-19 fail to induce the long-lasting, ligand-bound desensitized state of GluR5-2a receptors observed with DH, neoDH, and 8-deoxy-neoDH (Swanson et al., 1997;Sanders et al., 2005).

C8 and C9 Epimers Have Reduced Affinity for KAR Subunits

To test the importance of the spatial orientation of the critical C8 and C9 substituents in conferring selectivity for KARs, we first determined the affinities of the C8 and C9 epimers on KAR and AMPAR subunits in radioligand binding assays (Table 1; Fig. 5). The single C8 epimer, 8-epi-neoDH, weakly displaced radiolabeled ligand from a number of KAR and AMPAR subunits (Table 1), but it had the highest affinity for GluR5-2a subunits (K_i = 34 nM; n = 3–5) (Fig. 5A, top left). 9-F-8-epi-neoDH, in which the C9 hydroxyl group was replaced with an electrophilic fluorine, also displaced [^{3}H]kainate selectively from GluR5-2a KAR subunits (K_i = 28 nM; n = 2–4). In single-point assays (at 10 μM) with other receptor subunits, displacement of radioligand with 9-F-8-epi-neoDH proved very similar to that of 8-epi-neoDH (Fig. 5A, top right). The C9 epimer, 9-epi-neoDH, displaced [^{3}H]kainate from GluR5-2a subunits (K_i = 292 nM; n = 3–4), with an affinity ~300-fold lower than neoDH, and it was inactive at other subunits (Fig. 5A, bottom left). Alteration of the spatial orientation of both the C8 and C9 groups in 8,9-epi-neoDH effectively eliminated affinity for all receptor subunits, including GluR5-2a (n = 3–4) (Table 1; Fig. 5A, bottom right). These data indicate that GluR5-2a is the only subunit that tolerates alteration of the spatial orientation of the C8 and C9 functional groups. As with the group 1 deoxy compounds, variation at C8 had less consequence on binding affinity for GluR5-2a compared with the critical C9 group.

In whole-cell patch-clamp recordings, 8-epi-neoDH, 9-F-8-epi-neoDH, and 9-epi-neoDH all elicited rapidly activating currents from GluR5-2a-expressing cells (Fig. 5B). 8-Epi-neoDH and 9-F-8-epi-neoDH (n = 4; 10 μM) elicited large desensitizing currents with variable kinetics; in contrast, 9-epi-neoDH (n = 3; 50 μM) elicited very small amplitude, weakly desensitizing currents relative to the glutamate-evoked controls. 8,9-Epi-neoDH failed to elicit a detectable current when applied to GluR5-2a-expressing cells at high test concentrations, but it modestly inhibited glutamate-evoked currents in GluR5-2a-expressing cells (data not shown); however, 8,9-epi-neoDH has a very low affinity for GluR5-2a KARs; thus, any agonist activity may be very weak. As a result, the pharmacological activities and receptor selectivity of these epimeric compounds were generally similar to those of their deoxy counterparts.

C2 and C4 Epimers Maintain Affinity for a Subset of Non-*N*-methyl-$_D$-aspartate Receptor Subunits

Uncontrolled chirality in the synthetic pathway for neoDH yielded two analogs of the marine toxin, 4-epi-neoDH and 2,4-epi-neoDH, in which the $_L$-glutamate backbone in neoDH had altered stereochemistry (Sakai et al., 2001a) (Fig. 1); therefore, they seemed unlikely to bind KARs with significant affinity. However, these molecules were weakly convulsant when injected i.c.v. (Shoji et al., 2006), suggesting that they might retain affinity for a subset of receptors. In binding studies, 2,4-epi-neoDH selectively displaced [^{3}H]kainate from GluR5-2a and GluR6a subunits (K_i = 2.4 and 7.7 μM, respectively; n = 3–4), with no detectable activity on other KAR or AMPAR subunits (>100 μM; n = 3–4) (Table 1; Fig. 6A). In contrast, 4-epi-neoDH bound to both GluR5-2a and GluR6a KAR subunits, with similar affinities relative to 2,4-epi-neoDH (K_i values of 559 nM and 6.7 μM, respectively; n = 3) (Table 1; Fig. 6B), but it also weakly displaced radioligand from other KA and AMPAR subunits (n = 3). Neither 2,4-epi-neoDH nor 4-epi-neoDH bound the GluR7 receptor appreciably. Thus, these molecules exhibit distinct pharmacological profiles, and 2,4-epi-neoDH in particular seems to have a level of KAR selectivity (over AMPA receptors) not observed previously.

The pharmacological activities of the C2/C4 epimers were determined in patch-clamp assays with GluR5-2a or GluR6a KARs and GluR4(i) AMPA receptors. Application of 2,4-epi-neoDH (100 μM) failed to elicit detectable current in either GluR5-2a or GluR6a-expressing cells (n = 3–5; Fig. 6, C and D); thus, it does not exhibit agonist activity. In contrast, a high

concentration (50 μM) of 4-epi-neoDH evoked small but detectable currents from GluR5-2a and GluR6a receptors (n = 3–6; Fig. 6, C and D).

2,4-Epi-neoDH exhibited antagonist activity; this was demonstrated by applying varying concentrations of 2,4-epi-neoDH before testing with glutamate in the continued presence of the analog. 2,4-Epi-neoDH at 30 μM reduced glutamate-induced currents from GluR5-2a receptors by ~70%, whereas the same concentration reduced glutamate-induced currents from GluR6a receptors by ~30% (Fig. 7A). In contrast, application of 300 μM 2,4-epi-neoDH failed to inhibit GluR4(i) AMPARs (Fig. 7A). Inhibition-response analysis revealed that IC_{50} values for 2,4-epi-neoDH were 7.5 and 74 μM on GluR5-2a and GluR6a receptors, respectively (n = 3 for each concentration; Fig. 7B). We noted that the data derived from recording of the GluR5-2a receptor was poorly fit by the single component logistic curve, particularly at the lower concentrations. This inconsistency may arise from intersubunit or interdimer cooperativity in the inhibitory activity or may be an apparent artifact resulting from run-down of the GluR5-2a receptor currents. In summary, these results demonstrate that 2,4-epi-neoDH is an antagonist (or possibly a very weak partial agonist) for these receptors.

We noted the receptor desensitization induced by application of either 2,4-epi-neoDH or 4-epi-neoDH was prolonged after a brief exposure to these ligands, demonstrating that these analogs had longer lasting interactions with the receptors than would be predicted by their relatively low binding affinities. This was evident in the attenuation of the peak current amplitudes in response to test applications of glutamate after application of the analogs. Figure 8 compares the run-down of the receptor currents (with no analog application) to the amplitude of glutamate-evoked currents preceding and in the 13 min after application to either GluR5-2a (n = 9; Fig. 8A) or GluR6a (n = 4; Fig. 8B) receptors. Both compounds remained associated with the GluR5-2a receptor for many minutes after analog application. Recovery from desensitization is marginally more rapid after 2,4-epi-neoDH (n = 3–6) compared with 4-epi-neoDH (n = 3–5); the latter analog additionally stabilizes a desensitized state of the receptor, as revealed by the incomplete recovery back to control levels (within the time scale of our experiment). In contrast, current amplitudes recovered more slowly after application of 2,4-epi-neoDH to GluR6a receptors (n = 3–6), and 4-epi-neoDH (n = 3–4) only exhibited a transient desensitization. These observations suggest that the analogs could be useful as functional antagonists for a subpopulation of kainate receptors.

Understanding Determinants of Receptor Selectivity Using Molecular Dynamics Simulations

To explain the analog specificity and selectivity, we carried MD simulations with ligands docked to the template GluR5:(*S*)-glutamate structure (Protein Data Bank 1YCJ; Naur et al., 2005). Figure 9 shows the results of our simulations, with Fig. 9A illustrating the orientation of the GluR5 ligand binding domain (LBD); the white box delineates the area of focus for Fig. 9, B and C.

In the first round of simulations, we explored why the binding affinity of 8-deoxy-neoDH to GluR6a receptors was reduced by >1000-fold compared with neoDH, but, in contrast, it maintained an equivalent affinity for GluR5-2a subunits (Table 1; Fig. 2). We previously carried out MD simulations with GluR5 and DH (Sanders et al., 2006), and similarly neoDH binding to the GluR5 LBD is probably stabilized through 1) canonical interactions between the glutamate backbone and conserved elements of the LBD; 2) interactions between the furopyran ring and Y489 and other hydrophobic binding pocket residues; and 3) polar contacts between the C8 and C9 hydroxyl groups and E738 (main chain N) and the S741 hydroxyl group, respectively. MD simulations suggest that 8-deoxy-neoDH retains a similar set of interactions and orientation in the LBD, with the obvious exception that the C8 hydroxyl-E738 polar interaction is lost (Fig. 9B, top). We postulate that the loss of affinity in the GluR6a LBD could be explained in two ways. First, a significantly weaker hydrogen bond could be formed

between the C9 hydroxyl and the threonine found at position 741 in GluR6 and GluR7 subunits. The additional methyl group in T741 potentially projects unfavorably toward N721 (S721 in GluR5), which probably stabilizes binding of ligand to these receptor subunits through interdomain contacts with E441. A second possible explanation is based on the closer hydrophobic packing observed in the simulations with 8-deoxy-neoDH compared with neoDH; it is possible that F735 in GluR6, which forms part of the pocket "wall," displaces a key water molecule that stabilizes ligand binding to GluR5 subunits (which have a less bulky leucine in the analogous position). Consistent with this hypothesis, introduction of bulkier groups at the 735 and 741 positions in the GluR5 LBD significantly reduced affinity for MSVIII-19, which also shows closer packing similar to that modeled with 8-deoxy-neoDH (Sanders et al., 2006).

Simulations were also used to investigate why 8-deoxy-neoDH and 9-deoxy-neoDH exhibited ~100-fold differences in affinity for the GluR5 subunit. As shown in Fig. 9B, bottom, the MD simulations stabilized the ring structure of 9-deoxy-neoDH in an orientation that forced the C8 hydroxyl into nearly the same space as the C9 hydroxyl group in 8-deoxy-neoDH, which thereby facilitated the formation of the hydrogen bond with S741. As a result, we postulate that it is the loss of favorable hydrophobic packing with Y489 and other S1 residues that primarily reduces the affinity of 9-deoxy-neoDH for GluR5-2a. As well, the position of the γ-carboxyl group is rotated in 9-deoxy-neoDH relative to 8-deoxy-neoDH, which potentially disrupts a stabilizing network of hydrogen bonds with water molecules and the main chain amine of E738.

Finally, we performed MD simulations with 2,4-epi-neoDH, the novel GluR5-2a and GluR6a antagonist. This structure was significantly less stable than others in the simulations, as would be expected from the low affinity and predicted loss of one or more of the interactions between the glutamate congener and three residues conserved in all KAR ligand binding domains (Mayer, 2005; Nanao et al., 2005; Naur et al., 2005). We were surprised to find that many of these canonical bonds were maintained, although it is likely that the reduced affinity of the ligand results from a weakening of the bond strength (Fig. 9C). Interactions between the α-carboxyl and R523 and S689 were observed in the MD simulation, for example, as was the γ-carboxyl-T690 contact. Most notably, the altered chirality flipped the orientation of the ring structure, greatly reducing the favorable hydrophobic interactions with S1 residues and displacing the critical water molecule that stabilizes binding of other analogs near L735. It is likely that the affinity is reduced for all the receptor subunits by projection of the residue at position 721 (serine in GluR5, asparagine in GluR6 and GluR7) into the C8 hydroxyl group. The basis for the weak affinity for GluR5-2a and GluR6a probably lies in the interaction between C8 and C9 hydroxyls with Y489 and E441. The 2,4-epi-neoDH-GluR5 model structure is significantly more open relative to the glutamate-bound structure (i.e., the domains exhibit less rotation around the central hinge region), consistent with its antagonist activity.

In summary, these simulations yield insight into the molecular interactions that play a role in determining ligand affinity and activity. Furthermore, they may be useful for future synthetic efforts to improve specificity for KAR subunits such as GluR6.

Discussion

Kainate receptors primarily subserve modulatory functions in the brain, and for that reason they may represent approachable targets for therapeutic manipulation in several neurological diseases. Development of a wider variety of pharmacological tools that act on KARs will be particularly useful for exploring their utility as drug targets. Toward that end, here we extended our previous studies on analogs of the natural marine toxins dysiherbaine and neodysiherbaine

to characterize further the structural basis for specificity and activity at KARs (Sanders et al., 2005, 2006).

Our primary findings from the current study are 4-fold. First, we determined that the stereochemistry of the C8 and C9 hydroxyl groups was a critical determinant of affinity for all receptor subunits except GluR5-2a, which was relatively insensitive to changes in orientation unless both hydroxyl groups were altered. Second, we found that the change in affinity for KARs observed with MSVIII-19 (8,9-dideoxy-neoDH), relative to the parent compound neoDH, is largely accounted for by loss of the C9 hydroxyl group. However, unlike MSVIII-19, 9-deoxy-neoDH remained an agonist, which probably underlies its more potent convulsant activity (Shoji et al., 2006). Third, two new compounds, 2,4-epi-neoDH and 4-epi-neoDH, were found to have novel pharmacological profiles; furthermore, the former compound acts as a GluR5-2a- and GluR6a-selective KAR antagonist. Fourth, we observed a surprising dissociation between the relatively low-binding affinity of 2,4-epi-neoDH and 4-epi-neoDH for the GluR5-2a subunit and a prolonged association in a stable, ligand-bound desensitized state in physiological studies. These results suggest that the conformational state measured in the equilibrium binding assays does not represent the highest affinity state stabilized by the compound and that these analogs could represent effective functional antagonists at concentrations significantly lower than that required for receptor activation. In summary, our results provide several new insights into the molecular basis for specificity and selectivity of these compounds, and they suggest that the 2,4-epi-neoDH and 4-epi-neoDH molecules represent new templates for synthetic manipulation that could lead to novel pharmacological profiles of KAR antagonism.

Divergence in Binding Affinity and Functional Activity: What Interactions Underlie Agonism and Antagonism?

Our previous studies demonstrated that MSVIII-19, or 8,9-dideoxy-neoDH, is a high-affinity antagonist for GluR5 receptors, but MD simulations supported a relatively closed structure similar to that observed with agonists (Sanders et al., 2005, 2006). It is notable that the K_i of MSVIII-19 was significantly higher than its potency for inhibition of glutamate-evoked currents from GluR5 receptors (K_i = 128 nM; IC_{50} = 23 nM) (Sanders et al., 2005). One of our objectives in the current study was to compare the activity of intermediate analogs that had only a single hydroxyl group removed, which we anticipated would lend insight into the unusual behavior of MSVIII-19. The binding affinity of 9-deoxy-neoDH closely matches that of MSVIII-19, as does its ability to inhibit glutamate-evoked currents by pre-desensitizing GluR5 receptors, suggesting that the pharmacological profile of MSVIII-19 for GluR5 KAR subunits results primarily from the loss of the C9 hydroxyl group. However, in functional assays 9-deoxy-neoDH acts as an agonist, whereas MSVIII-19 is an antagonist, and it is likely that this agonist activity underlies the higher seizurogenic activity of 9-deoxy-neoDH (Shoji et al., 2006). Thus, we postulate that the interaction between the C8 hydroxyl group in 9-deoxy-neoDH, or more potently, the C9 hydroxyl in 8-deoxy-neoDH, and S741 in the LBD underlies the difference in agonist versus antagonist activity of these compounds. Finally, it is apparent that the high-affinity, desensitized functional state promoted by low concentrations of 9-deoxy-neoDH, for example, does not necessarily correspond to the conformation of the receptors assumed during equilibrium binding experiments, because of the divergence in binding affinity and potency of inhibition.

A similar divergence in apparent affinity and functional activity was noted for the 4-epi-neoDH molecule. The K_i value of ~560 nM for GluR5-2a receptors suggests that the interaction is of rather low affinity, but this is belied by the markedly long duration of inhibition of glutamate-evoked currents (Fig. 8). We conclude that the inhibitory activity exhibited by 4-epi-neoDH arises from prolonged and stable binding to the desensitized state of the receptor; a similar but

significantly longer lasting activity was first observed with the high-affinity agonist DH, which desensitizes GluR5-2a receptors irreversibly within the context of our physiological recordings (Swanson et al., 2002). In summary, the unique structures of a subset of DH, neoDH, and related analogs induce unusually stable desensitized states in KARs (primarily GluR5) that are preceded by varying degrees of receptor activation.

Activity at GluR5 Subunits Correlates with Seizure Activity

KARs agonists are known to be potent convulsants (Ben-Ari and Cossart, 2000), and DH, the first marine toxin isolated from *D. herbacea*, exhibits the most potent seizurogenic activity of any excitatory amino acid (Sakai et al., 1997). Most of the subsequent analogs of DH elicit varying degrees of convulsant behaviors; MSVIII-19, as an exception, produced subseizure-stereotyped behavior followed by unresponsiveness (Sasaki et al., 1999; Sakai et al., 2001a). 8,9-Epi-neoDH also fails to elicit convulsive behavior even at high doses, probably due to its very low affinity for KARs. Given that the analogs exhibit a range of seizure potencies and binding affinities, we attempted to determine whether these two parameters were strongly correlated. As shown in Fig. 10, we found that the affinity for GluR5-2a KAR subunits and convulsant activity of a range of compounds, as indicated by ED_{50} values upon i.c.v. injection in mice, were highly correlated ($r = 0.89$; $p < 0.01$). In contrast, a weaker correlation was observed between seizure activity and binding affinity for GluR6a subunits ($r = 0.74$; $p = 0.095$), and this lower correlation is an overestimate given that many analogs could not be included in the analysis because they showed no affinity for the GluR6a subunit. No apparent correlations were possible with GluR7a, KA2, or AMPA receptor binding because these subunits in large part did not interact with the analogs. This relationship strongly supports the hypothesis that activation of GluR5-containing receptors, which in the hippocampus predominantly reside on interneurons, underlies convulsant activity. Efficacy as GluR5 agonists probably further contributes to the seizurogenic potency of the analogs characterized within this study, particularly because the analogs show varied functional behavior with some acting as very weak partial agonists (i.e., 9-epi-neoDH) and others acting as full agonists or highly efficacious partial agonists (i.e., 8-deoxy-neoDH). This could be the case for the C2/C4 epimer analogs, which have generally similar binding profiles but notable differences in their potency for seizure induction. 2,4-epi-neoDH binds GluR5-2a receptors, with a K_i of 2.4 μM, and it has an ED_{50} of 11.4 nmol/mouse, whereas 4-epi-neoDH binds GluR5-2a receptors with slightly higher affinity (K_i = 559 nM), but it has an ED_{50} that is >6-fold lower than that of 2,4-epi-neoDH (ED_{50} of 4-epi-neoDH = 1.7 nmol/mouse). The most notable difference between these two analogs is their efficacy as agonists, in that 4-epi-neoDH elicits large currents from both GluR5-2a and GluR6a receptors, whereas 2,4-epi-neoDH fails to activate GluR5 or GluR6 receptors, even at 100 μM, and rather acts as a antagonist. Thus, GluR5-2a agonist efficacy may be an important factor, in addition to binding affinity for receptor subunits, in the seizure potency of these analogs.

This correlation supports the development of GluR5-selective antagonists as potential anticonvulsant compounds. The efficacy of this strategy was demonstrated in studies in which two GluR5 subunit-selective antagonists, LY377770 and LY382884, prevented induction and maintenance of seizure activity in multiple models of epilepsy (Smolders et al., 2002). More recently, aberrant KAR signaling was shown to contribute to hyperexcitability after seizurogenesis, and this activity was attenuated by desensitization of KARs (Epsztein et al., 2005); however, the subunit composition of the receptors involved in this process were not identified pharmacologically. In some respects, the strong correlation with GluR5 binding was a surprise, because a number of studies suggest that GluR6-containing receptors are the predominant targets of KAR agonists that lead to convulsions. In particular, gene targeting of the GluR6 subunit attenuates susceptibility to kainate-induced seizures (Mulle et al., 1998; Fisahn et al., 2004). It is possible that the specificity of the neoDH analogs for GluR5 receptors

elicits seizurogenesis through distinct mechanisms than kainate, which is relatively nonselective and will activate all kainate and AMPA receptors (depending on the concentration). In any case, our results further demonstrate that selective activation of GluR5-containing receptors produces seizures. It will be of interest to determine how this induction process occurs within the brain.

In summary, this characterization of neoDH analogs offers further insight into the determinants of activity and subunit selectivity for KAR subunits. Slight structural modifications of the parent molecule generated compounds with novel pharmacological profiles. In particular, 2,4-epi-neoDH is the first compound to act as a functional antagonist selective for GluR5- and GluR6-containing receptors without concurrent activity on AMPA receptors. We suggest that this compound will serve as a useful tool for further study of KARs in synaptic physiology and pathological conditions.

Acknowledgments

CSC, the Finnish IT Center for Science (Espoo, Finland), is acknowledged for the access to the computational resources (project jyy2516).

This study was supported by Kirschstein National Research Service Award F31 NS052007 (to J.M.S.), funds from the National Graduate School in Informational and Structural Biology (to P.P.), the Sigrid Jusélius Foundation (to O.T.P.), grant-in aid for scientific research awards from the Japanese Ministry of Education, Culture, Sports, Science and Technology (16073202 and 17380125 to Ma.S. and R.S., respectively), and the National Institute for Neurological Diseases and Stroke Grant R01 NS44322 (to G.T.S.).

ABBREVIATIONS

KAR	kainate receptor
GluR	glutamate receptor
KA	kainate
AMPAR	*α*-amino-3-hydroxy-5-methyl-4-isoxazolepropionic acid receptor
DH	dysiherbaine
AMPA	*α*-amino-3-hydroxy-5-methyl-4-isoxazolepropionic acid
neoDH	neodysiherbaine
MSVIII-19	(2*R*,3*aR*,7*aR*)-2-[(2*S*)-2-qmino-2-carboxyl-ethyl]-hexahydro-furo[3,2-*b*] pyran-2-carboxylic acid
HEK	human embryonic kidney
iGluR	ionotropic glutamate receptor
MD	molecular dynamics
LBD	ligand binding domain
NS-102	5-nitro-6,7,8,9-tetrahydrobenzo[g]indole-2,3-dione-3-oxime
LY377770	3*S*,4*aR*,6*S*,8*aR*-6-(((1*H*-tetrazol-5-ylmethyl)oxy)methyl)-1,2,3,4,4*a*, 5,6,7,8,8*a*-decahydroisoquinoline-3-carboxylic acid
LY382884	3*S*,4*aR*,6*S*,8*aR*-6-((4-carboxyphenyl)-methyl)-1,2,3,4,4*a*,5,6,7,8,8*a*-decahydroisoquinoline-3-carboxylic acid

References

Alt A, Weiss B, Ornstein PL, Gleason SD, Bleakman D, Stratford RE Jr, Witkin JM. Anxiolytic-like effects through a GLU(K5) kainate receptor mechanism. Neuropharmacology 2007;52:1482–1487. [PubMed: 17418283]

Ben-Ari Y, Cossart R. Kainate, a double agent that generates seizures: two decades of progress. Trends Neurosci 2000;23:580–587. [PubMed: 11074268]

Christensen JK, Varming T, Ahring PK, Jorgensen TD, Nielsen EO. In vitro characterization of 5-carboxyl-2,4-di-benzamidobenzoic acid (NS3763), a noncompetitive antagonist of GLUK5 receptors. J Pharmacol Exp Ther 2004;309:1003–1010. [PubMed: 14985418]

Dolman NP, More JC, Alt A, Knauss JL, Pentikäinen OT, Glasser CR, Bleakman D, Mayer ML, Collingridge GL, Jane DE. Synthesis and pharmacological characterization of N3-substituted willardiine derivatives: role of the substituent at the 5-position of the uracil ring in the development of highly potent and selective GLUK5 kainate receptor antagonists. J Med Chem 2007;50:1558–1570. [PubMed: 17348638]

Epsztein J, Represa A, Jorquera I, Ben-Ari Y, Crepel V. Recurrent mossy fibers establish aberrant kainate receptor-operated synapses on granule cells from epileptic rats. J Neurosci 2005;25:8229–8239. [PubMed: 16148230]

Filla SA, Winter MA, Johnson KW, Bleakman D, Bell MG, Bleisch TJ, Castano AM, Clemens-Smith A, del Prado M, Dieckman DK, et al. Ethyl (3S,4aR,6S,8aR)-6-(4-ethoxycarbonylimidazol-1-ylmethyl)decahydroiso-quinoline-3-carboxylic ester: a prodrug of a GluR5 kainate receptor antagonist active in two animal models of acute migraine. J Med Chem 2002;45:4383–4386. [PubMed: 12238915]

Fisahn A, Contractor A, Traub RD, Buhl EH, Heinemann SF, McBain CJ. Distinct roles for the kainate receptor subunits GluR5 and GluR6 in kainate-induced hippocampal gamma oscillations. J Neurosci 2004;24:9658–9668. [PubMed: 15509753]

Frisch, MJ.; Trucks, GW.; Schlegel, HB.; Scuseria, GE.; Robb, MA.; Cheeseman, JR.; Montgomery, JA., Jr; Vreven, T.; Kudin, KN.; Burant, JC., et al. Gaussian 03. Gaussian, Inc.; Wallingford, CT: 2004.

Herb A, Burnashev N, Werner P, Sakmann B, Wisden W, Seeburg PH. The KA-2 subunit of excitatory amino acid receptors shows widespread expression in brain and forms ion channels with distantly related subunits. Neuron 1992;8:775–785. [PubMed: 1373632]

Hollmann M, Heinemann S. Cloned glutamate receptors. Annu Rev Neurosci 1994;17:31–108. [PubMed: 8210177]

Jones G, Willett P, Glen RC, Leach AR, Taylor R. Development and validation of a genetic algorithm for flexible docking. J Mol Biol 1997;267:727–748. [PubMed: 9126849]

Kew JN, Kemp JA. Ionotropic and metabotropic glutamate receptor structure and pharmacology. Psychopharmacology 2005;179:4–29. [PubMed: 15731895]

Lerma J. Kainate receptor physiology. Curr Opin Pharmacol 2006;6:89–97. [PubMed: 16361114]

Lerma J, Paternain AV, Rodriguez-Moreno A, Lopez-Garcia JC. Molecular physiology of kainate receptors. Physiol Rev 2001;81:971–998. [PubMed: 11427689]

Mayer ML. Crystal structures of the GluR5 and GluR6 ligand binding cores: molecular mechanisms underlying kainate receptor selectivity. Neuron 2005;45:539–552. [PubMed: 15721240]

Mulle C, Sailer A, Pérez-Otaño I, Dickinson-Anson H, Castillo PE, Bureau I, Maron C, Gage FH, Mann JR, Bettler B, et al. Altered synaptic physiology and reduced susceptibility to kainate-induced seizures in GluR6-deficient mice. Nature 1998;392:601–605. [PubMed: 9580260]

Nanao MH, Green T, Stern-Bach Y, Heinemann SF, Choe S. Structure of the kainate receptor subunit GluR6 agonist-binding domain complexed with domoic acid. Proc Natl Acad Sci U S A 2005;102:1708–1713. [PubMed: 15677325]

Naur P, Vestergaard B, Skov LK, Egebjerg J, Gajhede M, Kastrup JS. Crystal structure of the kainate receptor GluR5 ligand-binding core in complex with (S)-glutamate. FEBS Lett 2005;579:1154–1160. [PubMed: 15710405]

Paternain AV, Vicente A, Nielsen EO, Lerma J. Comparative antagonism of kainate-activated kainate and AMPA receptors in hippocampal neurons. Eur J Neurosci 1996;8:2129–2136. [PubMed: 8921304]

Pentikäinen U, Pentikäinen OT, Mulholland AJ. Cooperative symmetric to asymmetric conformational transition of the apo-form of scavenger decapping enzyme revealed by simulations. Proteins 2007;70:498–508.

Pentikäinen U, Settimo L, Johnson MS, Pentikäinen OT. Subtype selectivity and flexibility of ionotropic glutamate receptors upon antagonist ligand binding. Org Biomol Chem 2006;4:1058–1070. [PubMed: 16525550]

Phillips JC, Braun R, Wang W, Gumbart J, Tajkhorshid E, Villa E, Chipot C, Skeel RD, Kale L, Schulten K. Scalable molecular dynamics with NAMD. J Comput Chem 2005;26:1781–1802. [PubMed: 16222654]

Pinheiro P, Mulle C. Kainate receptors. Cell Tissue Res 2006;326:457–482. [PubMed: 16847640]

Sakai R, Kamiya H, Murata M, Shimamoto K. Dysiherbaine: a new neurotoxic amino acid from the micronesian marine sponge Dysidea herbacea. J Am Chem Soc 1997;119:4112–4116.

Sakai R, Koike T, Sasaki M, Shimamoto K, Oiwa C, Yano A, Suzuki K, Tachibana K, Kamiya H. Isolation, structure determination, and synthesis of neodysiherbaine A, a new excitatory amino acid from a marine sponge. Org Lett 2001a;3:1479–1482. [PubMed: 11388846]

Sakai R, Swanson GT, Shimamoto K, Green T, Contractor A, Ghetti A, Tamura-Horikawa Y, Oiwa C, Kamiya H. Pharmacological properties of the potent epileptogenic amino acid dysiherbaine, a novel glutamate receptor agonist isolated from the marine sponge *Dysidea herbacea*. J Pharmacol Exp Ther 2001b;296:650–658. [PubMed: 11160654]

Sanders JM, Ito K, Settimo L, Pentikäinen OT, Shoji M, Sasaki M, Johnson MS, Sakai R, Swanson GT. Divergent pharmacological activity of novel marine-derived excitatory amino acids on glutamate receptors. J Pharmacol Exp Ther 2005;314:1068–1078. [PubMed: 15914675]

Sanders JM, Pentikäinen OT, Settimo L, Pentikäinen U, Shoji M, Sasaki M, Sakai R, Johnson MS, Swanson GT. Determination of binding site residues responsible for the subunit selectivity of novel marine-derived compounds on kainate receptors. Mol Pharmacol 2006;69:1849–1860. [PubMed: 16537793]

Sasaki M, Maruyama T, Sakai R, Tachibana K. Synthesis and biological activity of dysiherbaine model compound. Tetrahedron Lett 1999;40:3195–3198.

Shoji M, Akiyama N, Tsubone K, Lash LL, Sanders JM, Swanson GT, Sakai R, Shimamoto K, Oikawa M, Sasaki M. Total synthesis and biological evaluation of neodysiherbaine A and analogues. J Org Chem 2006;71:5208–5220. [PubMed: 16808508]

Smolders I, Bortolotto ZA, Clarke VR, Warre R, Khan GM, O'Neill MJ, Ornstein PL, Bleakman D, Ogden A, Weiss B, et al. Antagonists of GLU(K5)-containing kainate receptors prevent pilocarpine-induced limbic seizures. Nat Neurosci 2002;5:796–804. [PubMed: 12080343]

Swanson GT, Gereau RW IV, Green T, Heinemann SF. Identification of amino acid residues that control functional behavior in GluR5 and GluR6 kainate receptors. Neuron 1997;19:913–926. [PubMed: 9354337]

Swanson GT, Green T, Sakai R, Contractor A, Che W, Kamiya H, Heinemann SF. Differential activation of individual subunits in heteromeric kainate receptors. Neuron 2002;34:589–598. [PubMed: 12062042]

Valgeirsson J, Nielsen EO, Peters D, Mathiesen C, Kristensen AS, Madsen U. Bioisosteric modifications of 2-arylureidobenzoic acids: selective noncompetitive antagonists for the homomeric kainate receptor subtype GluR5. J Med Chem 2004;47:6948–6957. [PubMed: 15615543]

Valgeirsson J, Nielsen EO, Peters D, Varming T, Mathiesen C, Kristensen AS, Madsen U. 2-Arylureidobenzoic acids: selective noncompetitive antagonists for the homomeric kainate receptor subtype GluR5. J Med Chem 2003;46:5834–5843. [PubMed: 14667236]

Weiss B, Alt A, Ogden AM, Gates M, Dieckman DK, Clemens-Smith A, Ho KH, Jarvie K, Rizkalla G, Wright RA, et al. Pharmacological characterization of the competitive GLUK5 receptor antagonist decahydroisoquinoline LY466195 in vitro and in vivo. J Pharmacol Exp Ther 2006;318:772–781. [PubMed: 16690725]

Werner P, Voigt M, Keinaänen K, Wisden W, Seeburg PH. Cloning of a putative high-affinity kainate receptor expressed predominantly in hippocampal CA3 cells. Nature 1991;351:742–744. [PubMed: 1648176]

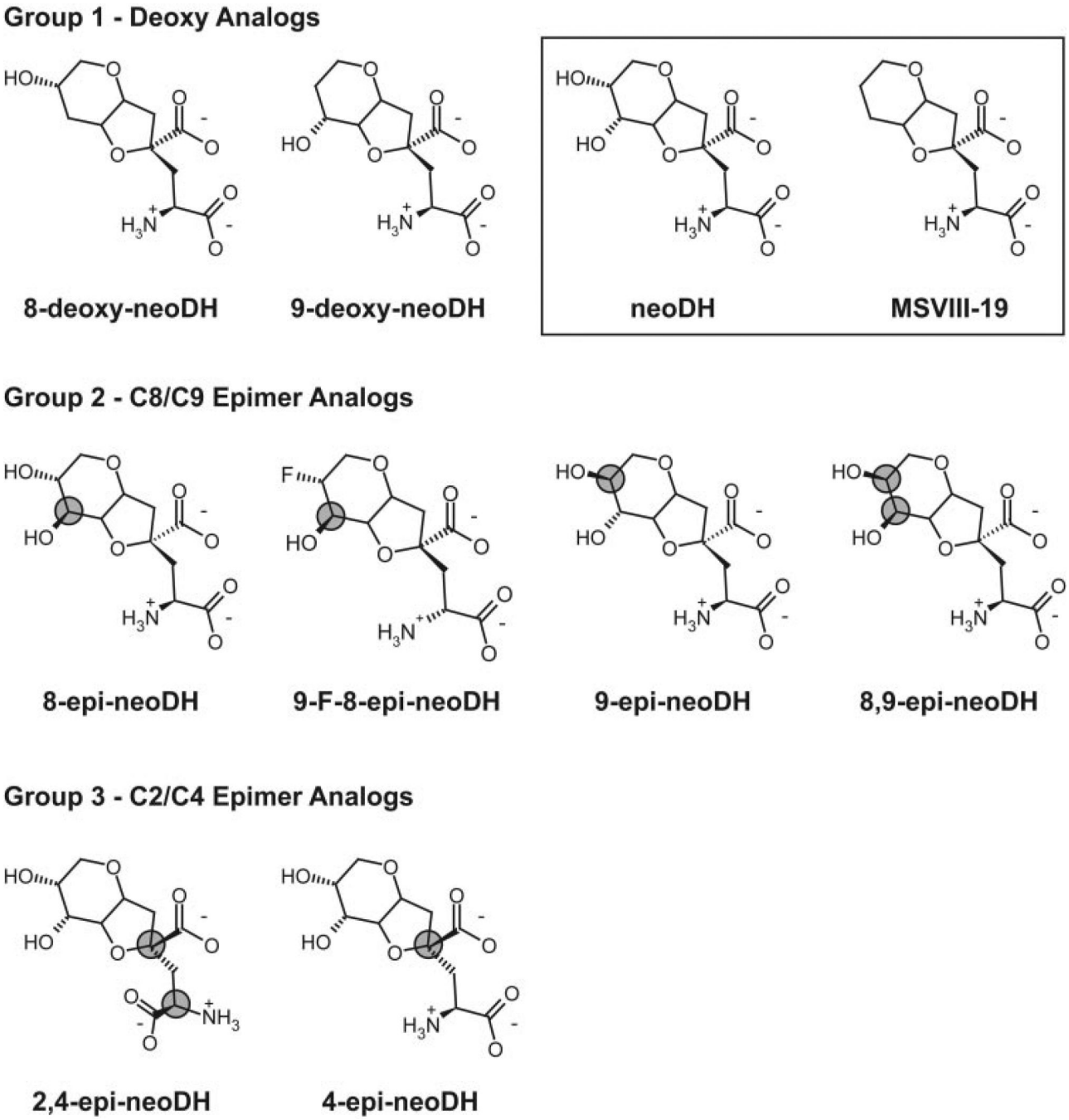

Fig. 1.

Chemical structures of the three groups of synthetic neodysiherbaine-derived analogs. The parent marine toxin neoDH and the first synthetic analog MSVIII-19 are outlined in a box in the first row of structures. neoDH contains a glutamate backbone connected to a rigid ring structure with hydroxyl groups at both the C8 and C9 ring positions; MSVIII-19 is the dideoxy synthetic analog. Group 1 analogs are the deoxy analogs at the C8 and C9 ring positions. Group 2 analogs are epimer analogs that manipulate the orientation of the substituents at the C8 and C9 ring positions. Group 3 analogs are epimer analogs at the C2/C4 positions within the glutamate backbone of the parent compound. The carbons changed are indicated by shaded gray circles.

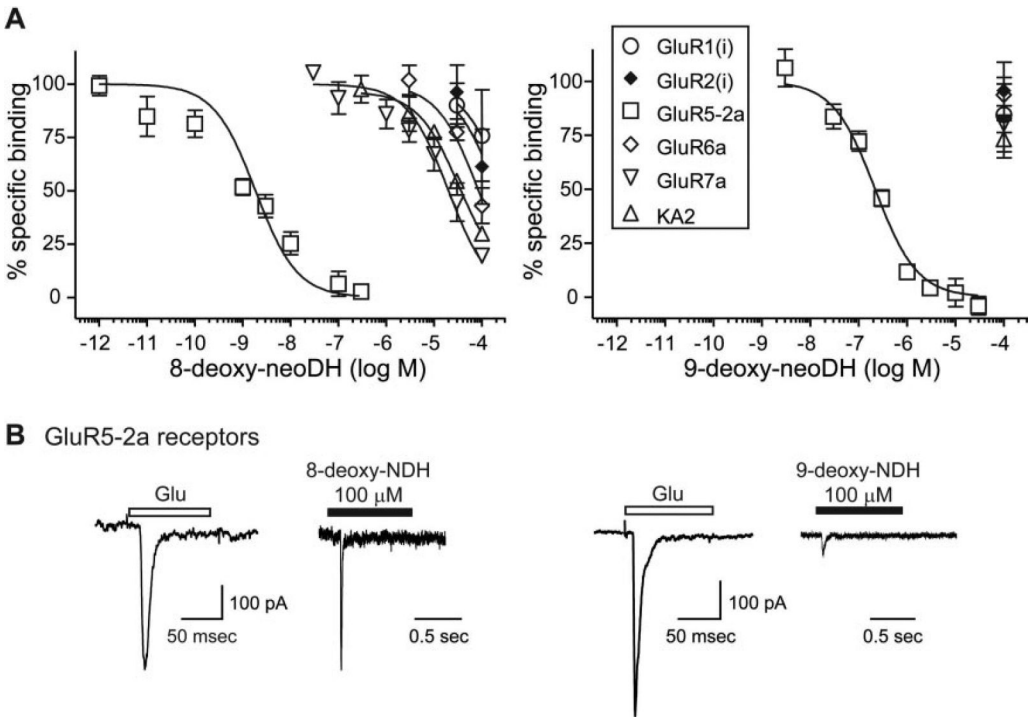

Fig. 2.

Deoxy analogs retain high affinity only for GluR5 subunits. A, displacement of [^{3}H]kainate and [^{3}H]AMPA from KA and AMPARs, respectively, for 8-deoxy-neoDH (left) and 9-deoxy-neoDH (right). Glutamate (1 mM) was used to determine nonspecific binding. Curves were fit with a one-site competition curve with fixed minima (0%) and maxima (100%). n = 3 to 5 for each concentration of analog on each receptor subunit. K_i values were calculated with the Cheng-Prusoff equation using the determined IC_{50} values and the radioligand K_d value (Table 1). B, both deoxy analogs are GluR5 agonists. Traces are representative of single control responses after 100-ms application of saturating concentrations of glutamate (10 mM) to GluR5-2a-expressing cells and analog-evoked currents during a 1-s application for 100 μM 8-deoxy-neoDH (left) and 100 μM 9-deoxy-neoDH (right).

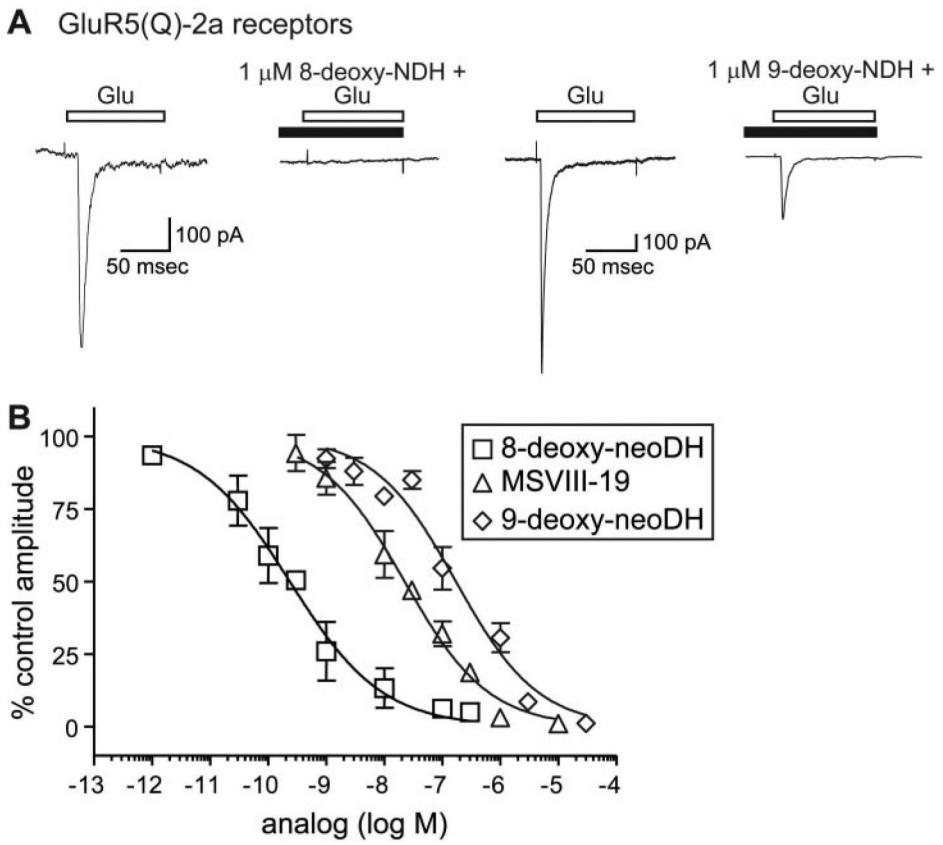

Fig. 3.

The deoxy analogs and MSVIII-19 differ in potency for pre-desensitization of GluR5-2a receptors. A, representative traces of glutamate-evoked currents (10 mM) before application of 1 μM 8-deoxy-neoDH (left) or 1 μM 9-deoxy-neoDH; subsequent glutamate-evoked currents in the presence of the analogs were attenuated by desensitization (right). B, inhibition-response curves for 8-deoxy-neoDH, 9-deoxy-neoDH, and MSVIII-19 (from Sanders et al., 2005) on recombinant GluR5-2a receptors. Logistic fits were constrained at the minima (0%) and maxima (100%), and IC_{50} values were determined to be 238 pM for 8-deoxy-neoDH and 151 and 23 nM for 9-deoxy-neoDH and MSVIII-19, respectively (Sanders et al., 2005), respectively. n = 3 to 5 for each concentration.

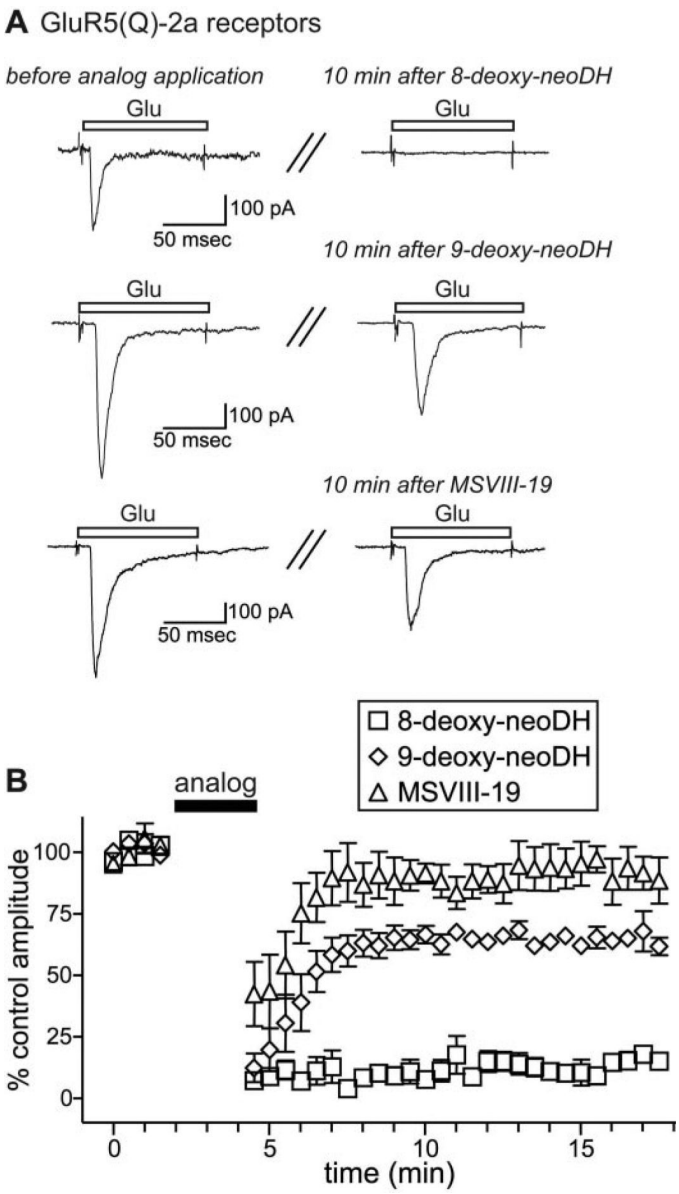

Fig. 4.

Recovery of glutamate-evoked currents after analog application is relatively rapid for 9-deoxy-neoDH and MSVIII-19. A, representative traces of control glutamate-evoked currents (left) before ~2.5-min application of 30 μM 8-deoxy-neoDH, 9-deoxy-neoDH, or MSVIII-19. Traces on the right are representative of glutamate-evoked currents 10 min after analog application. B, time course of recovery after application of 30 μM 8-deoxy-neoDH, 9-deoxy-neoDH, or MSVIII-19 on GluR5-2a-expressing cells. The graph shows relative peak amplitudes of glutamate-evoked currents (normalized to amplitudes during the 2-min control period) before and after application of the analogs (n = 3–6 at each time point). GluR5-2a receptors recovered from desensitization induced by 9-deoxy-neoDH and MSVIII-19 within 3 min, whereas 8-deoxy-neoDH remained associated beyond the duration of the experiments.

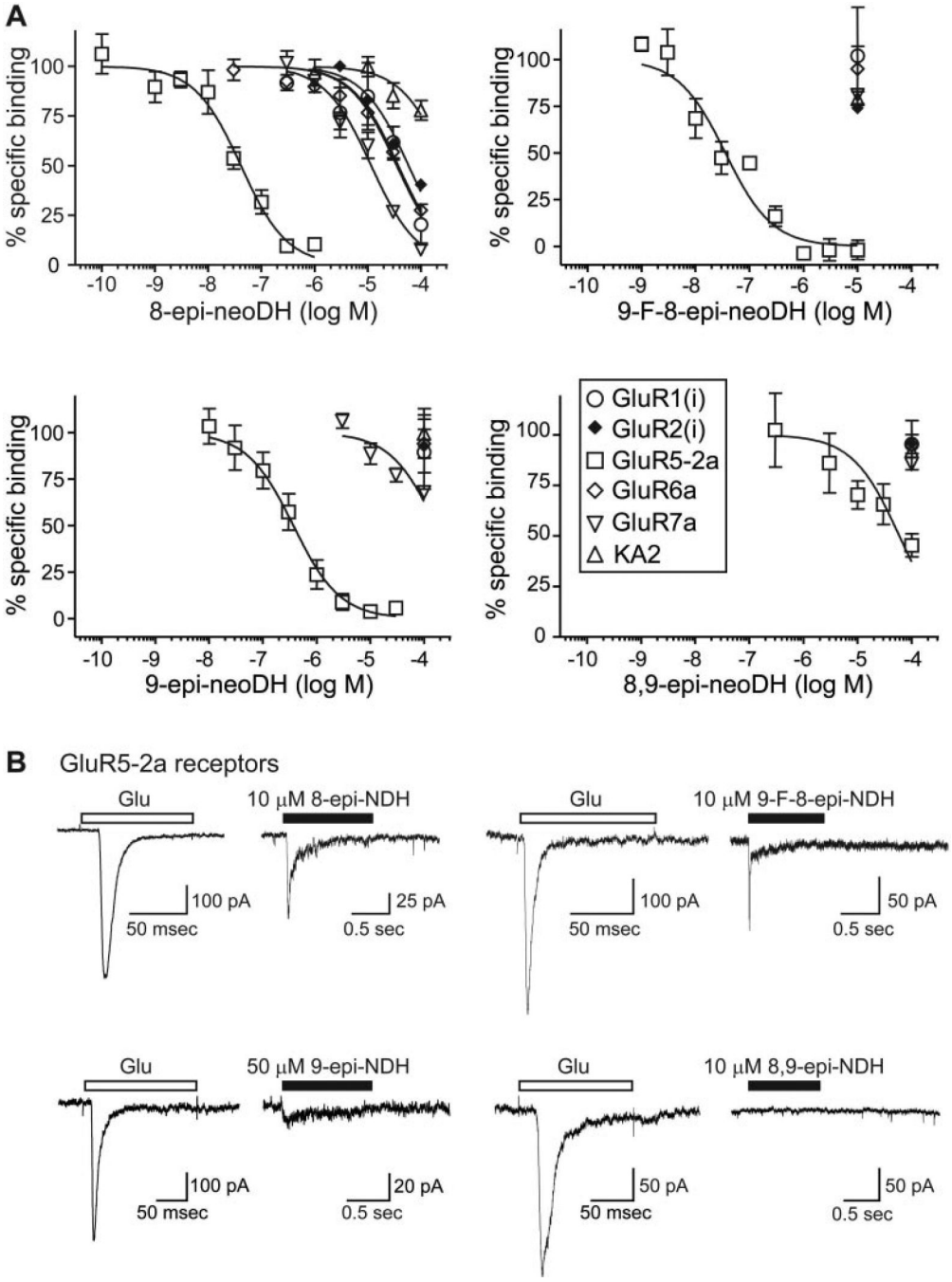

Fig. 5.

C8 and C9 epimers have reduced affinity for KAR subunits and are agonists. A, displacement of [^{3}H]kainate and [^{3}H]AMPA from KA and AMPARs, respectively, for 8-epi-neoDH, 9-F-8-epi-neoDH, 9-epi-neoDH, and 8,9-epi-neoDH. Glutamate (1 mM) was used to determine nonspecific binding. Curves were fit with a one-site competition curve with fixed minima (0%) and maxima (100%). n = 2 to 5 for each concentration of analog on each receptor subunit. K_i values were calculated with the Cheng-Prusoff equation using the determined IC_{50} values and the radioligand K_d value (Table 1). B, single C8/C9 epimer analogs activate GluR5-expressing cells. Traces are representative glutamate-evoked currents (10 mM) from GluR5-2a-expressing cells and analog-evoked currents during a 1-s application of 10 μM 8-epi-neoDH, 10 μM 9-

F-8-epi-neoDH, and 50 μM 9-epi-neoDH. 8,9-epi-neoDH at 10 μM fails to activate GluR5-2a-expressing cells.

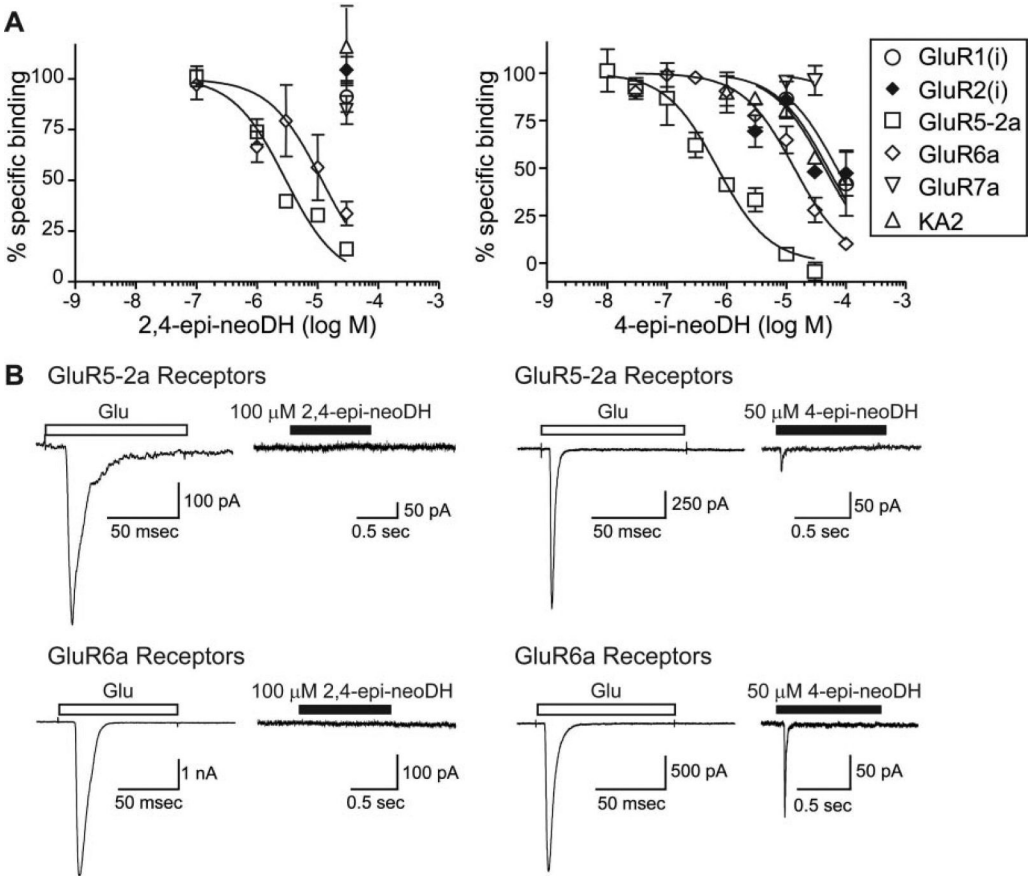

Fig. 6.

2,4-Epi-neoDH and 4-epi-neoDH maintain affinity for a subset of KAR subunits. A, displacement of [^{3}H]kainate and [^{3}H]AMPA from KA and AMPARs, respectively, for 2,4-epi-neoDH (left) and 4-epi-neoDH (right). Glutamate at 1 mM was used to determine nonspecific binding. Curves were fit with a one-site competition curve with fixed minima (0%) and maxima (100%). n = 3 to 5 for each concentration of analog on each receptor subunit. K_i values were calculated with the Cheng-Prusoff equation using the determined IC_{50} values and the radioligand K_d value (Table 1). B, 100 μM 2,4-epi-neoDH (1 s) fails to activate GluR5-2a or GluR6a receptors (left column). In contrast, 50 μM 4-epi-neoDH activates both GluR5-2a and GluR6a receptors (right column).

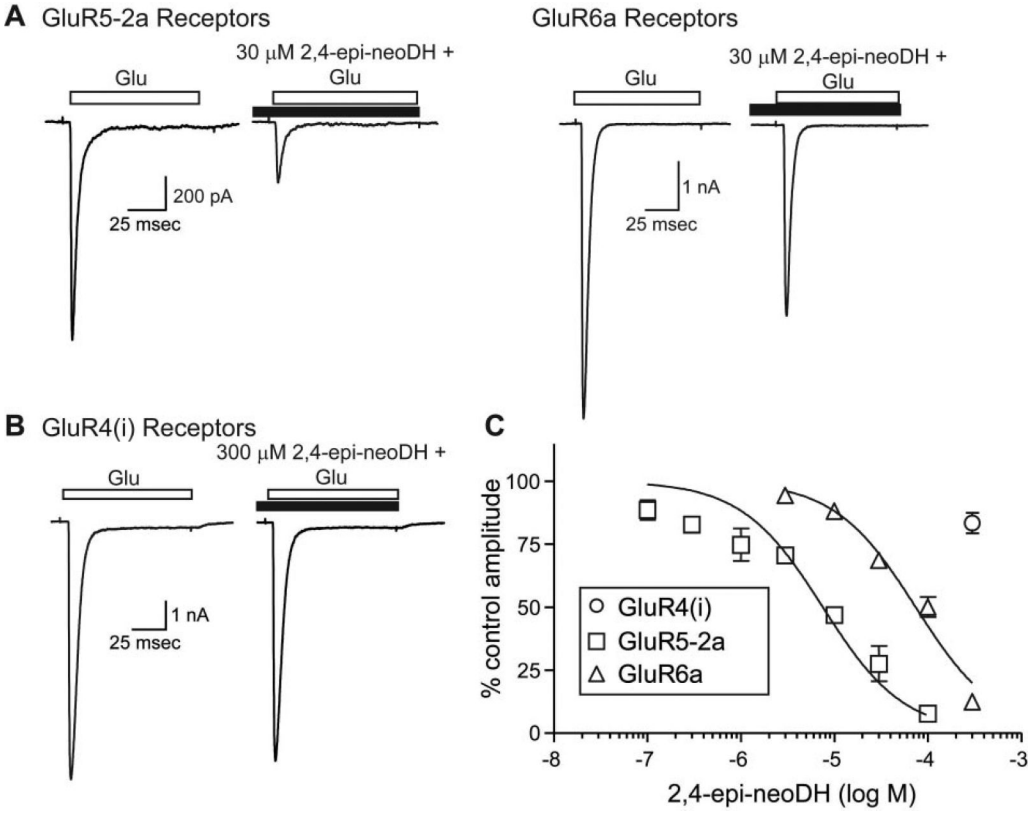

Fig. 7.

2,4-Epi-neoDH is a KAR antagonist. A, representative traces of glutamate-evoked currents (10 mM) from GluR5-2a and GluR6a receptors before application of 30 μM 2,4-epi-neoDH; subsequent glutamate-evoked currents in the presence of the analog were attenuated. B, currents from GluR4(i) receptors were not reduced by 300 μM 2,4-epi-neoDH. C, inhibition-response curves for 2,4-epi-neoDH on recombinant GluR4(i), GluR5-2a, and GluR6a receptors. Logistic fits were constrained to fixed minima (0%) and maxima (100%), and IC_{50} values were determined to be 7.5 and 74 μM for GluR5-2a and GluR6a receptors, respectively. n = 3 to 5 for each concentration.

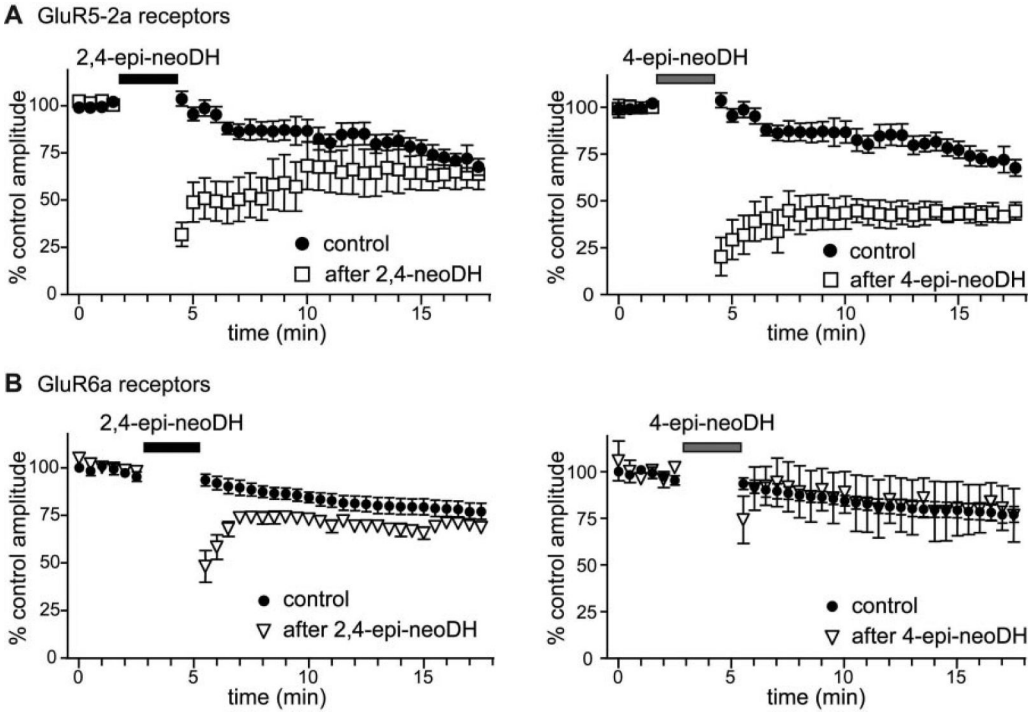

Fig. 8.

Low-affinity C2/C4 epimers have long-lasting inhibitory effects on glutamate-evoked currents. A, time course of recovery after application of 30 μM 2,4-epi-neoDH (left) and 30 μM 4-epi-neoDH (right) on GluR5-2a receptors. B, time course of recovery after application of the analogs to GluR6a receptors. The graphs show the normalized peak amplitudes of glutamate-evoked currents before and after analog application at the indicated times (n = 3–4 at each time point).

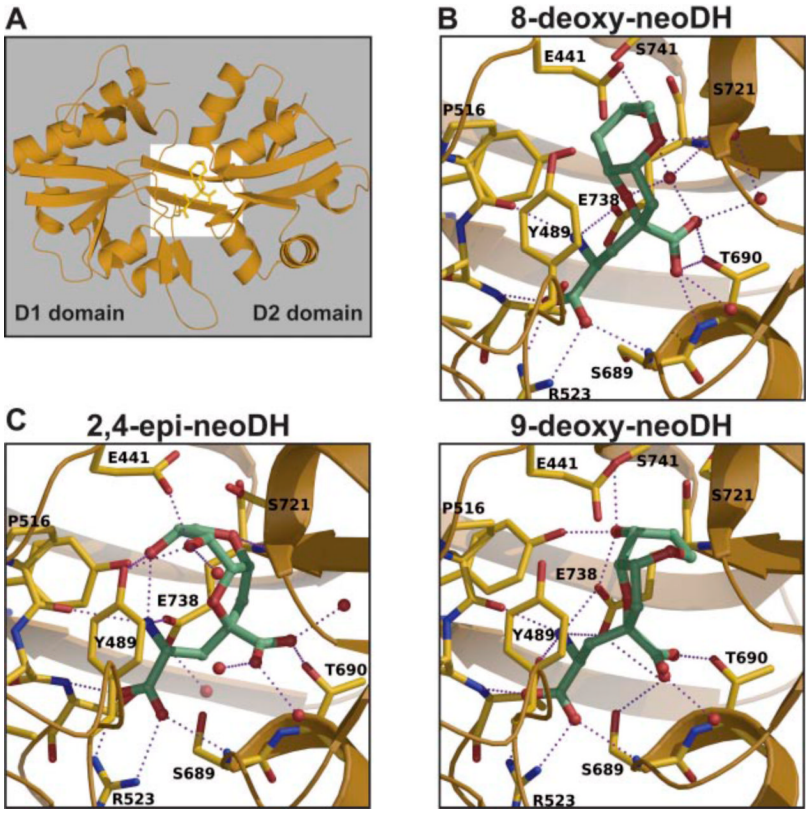

Fig. 9.

Molecular dynamics simulations of GluR5 with bound 8-deoxy-neoDH, 9-deoxy-neoDH, and 2,4-epi-neoDH. A, simulation of the GluR5 S1-S2 domain with 8-deoxy-neoDH, demonstrating the orientation of higher resolution images in the subsequent panels. Binding domains 1 and 2, consisting predominantly of S1 and S2 residues, respectively, are as indicated. B, model of 8-deoxy-neoDH (top) and 9-deoxy-neoDH (bottom) bound to GluR5. C, model of 2,4,-epi-neoDH bound to GluR5. Predicted water molecules and hydrogen bonds are shown in each panel. Detailed descriptions of the models are given in the text.

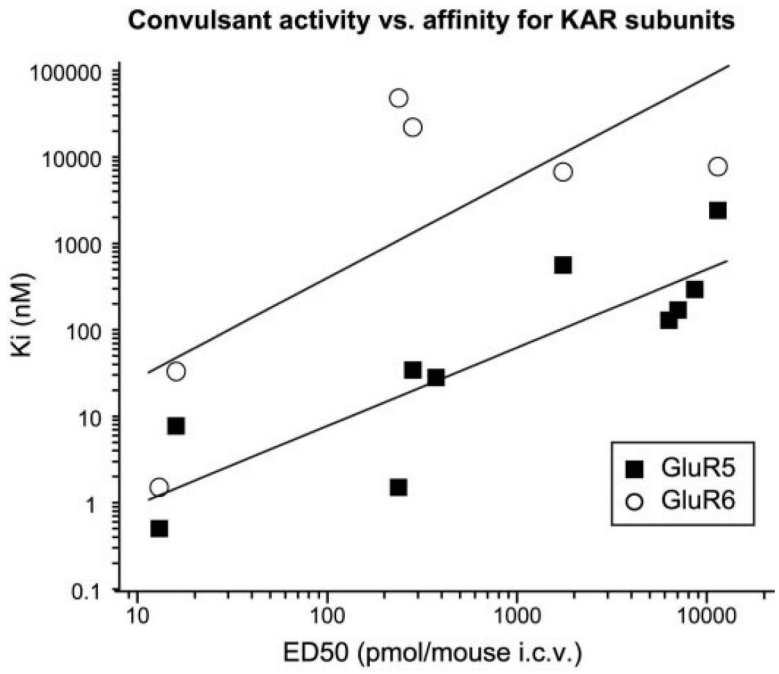

Fig. 10.

Binding affinity at GluR5-2a subunits correlates with seizure activity. Linear correlation graph is plotted as K_i (nanomolar) versus ED_{50} (picomoles per mouse) after i.c.v. injection of the following compounds: DH (13 pmol/mouse), neoDH (16 pmol/mouse), MSVIII-19 (6.3 nmol/mouse), 8-deoxy-neoDH (238 pmol/mouse), 9-deoxy-neoDH (7.1 nmol/mouse), 8-epi-neoDH (283 pmol/mouse), 9-epi-neoDH (8.6 nmol/mouse), 9-F-8-epi-neoDH (374 pmol/mouse), 2,4-epi-neoDH (11.4 nmol/mouse), and 4-epi-neoDH (1.7 nmol/mouse) (Shoji et al., 2006). These data show a correlation ($r = 0.86$; $p < 0.01$) for binding affinity of analogs for GluR5-2a KAR subunits. A much weaker correlation between seizure activity and binding affinity for GluR6a subunits of a subset of analogs was noted ($r = 0.74$; $p = 0.095$); several compounds could not be included in this analysis because they do not exhibit measurable affinity for this receptor subunit (i.e., MSVIII-19, 9-deoxy-neoDH, 9-epi-neoDH, and 9-F-8-epi-neoDH). Likewise, no correlation analysis was possible with GluR7a, KA2, or AMPA receptor subunits because of the absence of binding affinity.

TABLE 1

K_i values for displacement of [^{3}H]kainate and [^{3}H]AMPA by epimer and deoxy analogs of DH on KA and AMPAR subunits

K_i values were calculated using appropriate K_d values in the Cheng-Prusoff equation ($K_i = IC_{50}/(1 + [radioligand]/K_d)$). IC_{50} values were obtained using a one-site competition fit, with fixed minima (0%) and maxima (100%) using Prism 4 software. Nanomolar concentrations are in bold; all other concentrations are micromolar. K_i values are similar to those reported earlier for some of the compounds (Shoji et al., 2006), with the exception of 8-deoxy-neoDH, which was incorrectly reported to have a K_i value of 42 nM in the previous report.

	K_i Values of Epimer and Deoxy Analogs					
	GluR5-2a	**GluR6a**	**GluR7a**	**KA2**	**iGluR1**	**iGluR2**
Neodysiherbaine	**7.7**	**33**		0.6		
MSVIII-19	**128**	>100		>100	>100	>100
8-deoxy-neoDH	**1.5**	48	2.9	20	>100	>100
9-deoxy-neoDH	**169**	>100	>100	>100	>100	>100
8-epi-neoDH	**34**	22	1.7	>100	16	23
9-F-8-epi-neoDH	**28**	>100	>100	>100	>100	>100
9-epi-neoDH	**292**	>100	>100	>100	>100	>100
8,9-epi-neoDH	48	>100	>100	>100	>100	>100
2,4-epi-neoDH	2.4	7.7	>100	>100	>100	>100
4-epi-neoDH	**559**	6.7	>100	~30	>30	>30